Polyhedron 28 (2009) 665–672

Contents lists available at ScienceDirect

Polyhedron

journal homepage: www.elsevier.com/locate/poly

Concomitant polymorphism of an antiferromagnetically coupled dicopper(II,II) complex with single strand helical assembly: Synthesis, structure, DSC, magnetic and heterogeneous catalytic studies

Md. Mijanuddin [a], Atish Dipankar Jana [b], Michael G.B. Drew [c], Chang Seop Hong [d], Basab Chattopadhyay [e], Monika Mukherjee [e], Mahasweta Nandi [f], Asim Bhaumik [f], Madeline Helliwell [g], Golam Mostafa [h], Mahammad Ali [a,*]

[a] Department of Chemistry, Jadavpur University, Kolkata 700 032, India
[b] Department of Physics, Sripat Singh College, Jiaganj, Murshidabad, WB 742 123, India
[c] Department of Chemistry, University of Reading, Whiteknights, Reading, RG6 6AD, UK
[d] Department of Chemistry and Center for Electro- and Photo-Responsive Molecules, Korea University, Seoul 136-701, Republic of Korea
[e] Solid State Physics Department, Indian Association for the Cultivation of Science, Jadavpur, Kolkata 700 032, India
[f] Department of Materials Science and Centre for Advanced Materials, Indian Association for the Cultivation of Science, Jadavpur, Kolkata 700 032, India
[g] Department of Chemistry, University of Manchester, Manchester M13 9PL, UK
[h] Department of Physics, Jadavpur University, Kolkata 700 032, India

ARTICLE INFO

Article history:
Received 3 July 2008
Accepted 9 December 2008
Available online 11 February 2009

Keywords:
Cu^{II}-complexes
Concomitant polymorphism
Antiferromagnetically coupled
Immobilization
Hexagonal mesoporous silica
Heterogeneous catalysis
Epoxidation

ABSTRACT

Two concomitant polymorphic coordination complexes (dark blue – **I** and black – **II**) with the formula ($Cu_2C_{44}H_{60}N_4O_4$) have been synthesized and characterized crystallographically. Magnetic measurements show the presence of a strong antiferromagnetic interaction and the 2*J* value corresponds extremely well to the theoretically calculated one, indicating the fact that it follows nicely the magneto-structural relationship. Immobilization of the copper(II) complex **1** on a 2D-hexagonal mesoporous silica showed good catalytic efficiency in the liquid phase partial oxidation of olefins in the presence of TBHP as an oxidant.

1. Introduction

The designed synthesis of coordination complexes towards functional materials has become an active area of research during the last decade. Judicious choice of organic ligands and suitable transition metals has led to the controlled synthesis of transition metal complexes of different nuclearities with desired functionalities, such as catalytic activity, magnetism, non-linear optical properties, which have found promising industrial applications. Dinuclear copper complexes, in many cases, have shown interesting functional properties and the rational syntheses of these complexes have received current interest. Bulky Schiff-base ligands with O-donor atoms in many cases have been successfully used to control the synthesis of dinuclear copper complexes and phenolate/bis-phenolate ligands, in particular, have shown great promise towards this end [1–7].

Copper(II)–bisphenolate complexes are also important for their catalytic activity and during recent times they have been used as functional models of various biomolecules [1–6]; as a functional model of galactose oxidase (GO) [7], copper amine oxidases, etc. Immobilization of copper complexes over silica supports can be an effective methodology for the synthesis of active heterogeneous catalysts in the liquid phase partial oxidation of alkenes using peroxides as the oxidant [8,9]. The channels of hexagonal mesoporous silica (**HMS**) materials provide a confined space (2–50 nm) for stabilization and enhancement of the catalytic performance by influencing the chemo-, regio- and shape-selectivity of the reaction, and offer further opportunity to study "single molecular chemistry", which could take place in nano-restricted environments. Detailed studies of chemical reactions in a confined space would allow us to gain a fundamental understanding of the effects of local environment on the control of reaction pathways and the increase of product yield. A transition metal present at the surface of a mesoporous material with a very high surface area particularly showed excellent catalytic activity in liquid phase partial oxidation

* Corresponding author.
E-mail address: mali@chemistry.jdvu.ac.in (M. Ali).

0277-5387/$ - see front matter © 2009 Elsevier Ltd. All rights reserved.
doi:10.1016/j.poly.2008.12.047

reactions in the presence of *tert*-butyl hydroperoxide (TBHP) as an oxidant [10]. In the present contribution, we report the syntheses and crystal structures of two binuclear copper(II) complexes (**I** and **II**) of a tetra-coordinated amine-bisphenol ligand (H_2L), which are interestingly concomitant polymorphs. We have also shown that the immobilization of the soluble copper(II) complex **I** over highly ordered mesoporous silica resulted in a heterogeneous catalyst, which showed very good catalytic activity and epoxide selectivity in the oxidation of cyclohexene and styrene in the presence of TBHP as an oxidant. A low temperature magnetic study on complex **I** shows strong antiferromagnetic coupling between the two phenoxo-bridged Cu(II) centers.

H_2L

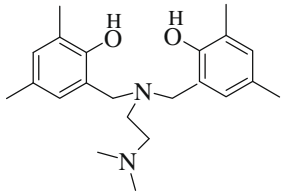

2. Experimental

2.1. Materials and methods

Starting materials for the synthesis of the ligand *N*,*N*-amine-bis(4,6-dimethylphenol)-*N*,*N*-dimethylethylenediamine(H_2L) viz 2,4-dimethylphenol (Lancaster), *N*,*N*-dimethylethylenediamine (Lancaster) and formaldehyde (E-Merck, Germany) were of reagent grade and were used without further purification. Solvents including acetone, methanol, dichloromethane (Merck, India) and triethylamine (SRL, India) were of reagent grade and were dried by standard methods before use. The hydrated salt of copper(II) acetate (A.R. Loba, India) was used as received.

2.1.1. Synthesis of the ligand (H_2L)

The ligand *N*,*N*-amine-bis(4,6-dimethylphenol)-*N*,*N*-dimethylethylenediamine (H_2L) was prepared by the reported method [11].

2.1.2. Synthesis of the complex [$Cu_2(L)_2$]

H_2L (0.356 gm, 1 mmol) dissolved in dry methanol/dichloromethane mixture (1:1, v/v) (20 ml) was refluxed with triethylamine (0.20 gm, 2 mmol) for 15 min to yield a yellow solution. To this solution was added $[Cu(OAc)_2] \cdot 2H_2O$ (0.20 gm, 1 mmol), and the solution was refluxed for another 5 h and filtered to remove the slight brown precipitate. Single-crystals were grown by slow evaporation at room temperature (~27 °C). The dark blue needle shape crystals (**I**) appeared within 2 days at the upper part of the vessel, while black block shape crystals (**II**) were obtained after 5 days (Fig. 1). Yield, black needles ~30%, dark blue blocks ~40%.

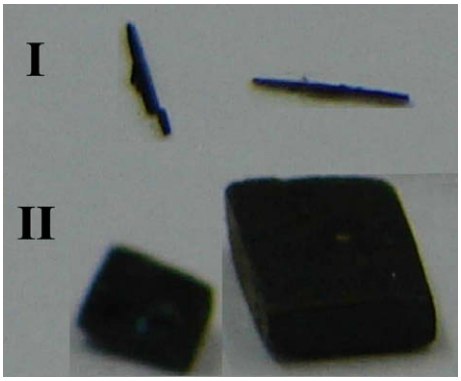

Fig. 1. Photograph of the two forms of $[Cu_2(L)_2]$ growing in $MeOH/CH_2Cl_2$ (1:1 v/v). Complex **I** gives needle-like crystals growing at the upper part of the beaker, while **II** is the block like crystals that grow at the lower part of the beaker.

Attempts to grow single-crystals at relatively low temperature (~5 °C) resulted in only **II** in 5–7 days, with no trace of **I**. *Anal.* Calc. for $C_{44}H_{60}Cu_2N_4O_4$ (836.06 g mol^{-1}): C, 63.21; H, 7.23; N, 6.70 Found: C, 62.94; H, 7.11; N, 6.41%. IR (cm^{-1}): 3423(br), 2993–2831(s), 1610(s), 1475(s), 1319(s), 1251(s), 858, 800.

2.2. Immobilization of complex **1** on 2D-hexagonal mesoporous silica

Highly ordered 2D-hexagonal mesoporous silica has been synthesized by using a mixture of cationic (cetyltrimethylammonium bromide, CTAB) and non-ionic (Brij-35, $C_{12}H_{25}$–$(OC_2H_4)_{23}$–OH, a polyether and aliphatic hydrocarbon chain) surfactant system as the supramolecular structure directing agent, by the method reported elsewhere [12]. This ordered mesoporous material was used as the catalyst support in this study. Immobilization of the metal complexes was carried out by dispersing 0.5 g of the mesoporous silica in a solution containing 120 mg of the metal complex dissolved in 25 ml dry acetonitrile. The resultant slurry was vigorously stirred at room temperature for 4 h. Then the solid was filtered, washed with acetonitrile and dried under vacuum. Hexagonal mesoporous silica and its corresponding immobilized analogs of **I** are designated as **HMS** and **HMS-Cu-I**, respectively. Both the host and the immobilized catalysts were characterized by powder XRD, electron microscopy and spectroscopic techniques.

2.3. Physical measurements

Elemental analyses were carried out using a Perkin–Elmer 240 elemental analyzer. The infrared spectrum (400–4000 cm^{-1}) was recorded from KBr pellets on a Nickolet Magna IR 750 series-II FTIR spectrophotometer. The variable-temperature magnetic susceptibility of complex **I** was performed using a SQUID magnetometer on a crystalline sample in the temperature range 300–2 K with an applied field of 0.5*T*. DSC thermograms were recorded on a Perkin–Elmer Pyris Diamond TGA/DTA thermal analyzer under a dynamic nitrogen environment.

2.4. X-ray crystallography

For complex **1**, data were measured at 293(2) K on a Bruker SMART APEX CCD area detector system [λ(Mo K_α) = 0.71073 Å], graphite monochromator with an ω-scan, crystal-detector distance 60 mm, collimator 0.5 mm. Data reduction by SAINTPLUS [13], absorption correction using an empirical method (SADABS) [14], structure solution using SHELXS-97 [15] and refined using SHELXL-97 [16]. All non-H atoms were refined anisotropically. Hydrogen atoms on the ligand were introduced in calculated positions and included in the refinement, riding on their respective parent atoms. For complex **II**, data were collected at 293(2) K with Mo K_α radiation using the MAR research image plate system positioning the crystals at 70 mm away from the image plate. One hundred frames were measured at 2° intervals with a counting time of 2 min. Data analysis was carried out with the XDS program [17]. The structure of **II** was solved by the direct method, and refined by full-matrix least-squares techniques on F^2 using SHELXS-97 [15] and SHELXL-97 [16]. The thermal parameters of all non-H-atoms were treated anisotropically. H-atoms were located from the difference Fourier map and refined isotropically. Crystal data for **I** and **II** are provided in Table 1.

Table 1
Crystal data and structure refinement for polymorphs **I** and **II**.

Parameters	Polymorph-**I**	Polymorph-**II**
Empirical formula	$C_{44}H_{60}Cu_2N_4O_4$	$C_{44}H_{60}Cu_2N_4O_4$
Formula weight	836.04	836.04
Temperature (K)	293	293
Wavelength (Å)	0.71073	0.71073
Crystal system	orthorhombic	orthorhombic
Space group	$P2_12_12_1$	*Pnna*
a (Å)	12.0097(16)	12.6479(6)
b (Å)	15.334(2)	14.1640(7)
c (Å)	23.780(3)	23.194(1)
V (Å^3)	4379.3(10)	4155.2(4)
Z, calculated density (Mg/m^3)	4, 1.268	4, 1.337
Absorption coefficient (mm^{-1})	1.048	1.070
F(000)	1768	1768
Crystal size (mm)	0.12 * 0.20 * 0.50	0.11 * 0.17 * 0.19
Crystal color	dark-blue	black
Crystal shape	needle	block
θ range for data collection (°)	1.6–25.0	1.76–26.40
Limiting indices	$-14 \leqslant h \leqslant 14$ $-18 \leqslant k \leqslant 18$ $-28 \leqslant l \leqslant 28$	$-15 \leqslant h \leqslant 15$ $-17 \leqslant k \leqslant 17$ $-29 \leqslant l \leqslant 28$
Reflections collected/unique [R_{int}]	42 266/7719 [0.049]	31 413/4264 [0.0244]
Data/restraints/parameters	6162/0/499	4264/0/364
Goodness-of-fit-on F^2	1.02	1.042
Final *R* indices [$I > 2\sigma(I)$]	$R_1 = 0.0384$, $wR_2 = 0.0956$	$R_1 = 0.0243$, $wR_2 = 0.0690$
Largest difference peak and hole (e Å^{-3})	0.38 and −0.17	0.334 and −0.222

Samples (**HMS** and **HMS-Cu-I**) were identified by powder XRD (PXRD) using a Seifert 3000P X-ray diffractometer on which small and wide-angle goniometers were mounted. The X-ray source was Cu K_α radiation (α = 0.15406 nm) with an applied voltage and current of 40 kV and 20 mA, respectively. Mesophases of different samples were analyzed using a JEOL, JEM 2010 TEM at an accelerating voltage of 200 kV. N_2 adsorption measurements were carried out using a Quantachrome Autosorb-1C-TCD at 77 K. Pre-treatment of the sample was done at 423 K for 3 h under high vacuum. For the Fourier transform infrared (FT-IR) measurement a Nicolet Magna IR 750 Series II was used. A Shimadzu AA-6300 double beam atomic absorption spectrophotometer was used for studying the loading of Cu through wet chemical analysis. UV–visible diffuse reflectance spectra for the immobilized catalysts were recorded on a Shimadzu 2401PC UV–visible spectrophotometer with an integrating sphere attachment using $BaSO_4$ as a background standard.

The oxidation reactions were carried out using 0.5 g of substrate and 0.10 g of loaded catalyst in 6 ml of CH_3CN under stirring in a two-neck round-bottom flask fitted with a water condenser and placed in an oil bath at 333 K. *tert*-Butylhydroperoxide (TBHP, 70 wt% aqueous, equimolar with respect to the substrate) was added immediately before the start of the reaction. Aliquots of the reaction mixture were withdrawn at various time intervals to study the progress of the reaction. In a typical operation, 0.5 cm^3 solution was taken out with the help of a micro-pipette and the solution was subjected to multiple ether extraction and the extract was concentrated. From this, 1 μl solution was withdrawn with the help of a gas tight syringe and injected to the GC port (Agilent 6890A, FID). For the identification of the products the GC retention times of different reaction products were compared with those of commercial standards.

3. Results and discussion

3.1. Structure of I and II

Both polymorphic forms, (**I**) and (**II**) (Figs. 2 and 3), of the title complex crystallize in the orthorhombic system with almost similar lattice constants (Table 1). The similarity of the unit cell dimensions of the two polymorphs suggests that the crystal structures of **I** and **II** are also related, although the space group for polymorph **I** is non-centrosymmetric, $P2_12_12_1$, with $Z = 4$, while that of polymorph **II** is a centric one, Pbnn, with $Z = 4$. Consequently, the asymmetric unit of **I** consists of a dinuclear Cu_2L_2 molecule with two phenolate O atoms acting as a $(\mu\text{-O})_2$ bridge between the metal centers. In **II**, however, only half of the complex molecule, i.e. a mononuclear CuL moiety, forms the asymmetric unit.

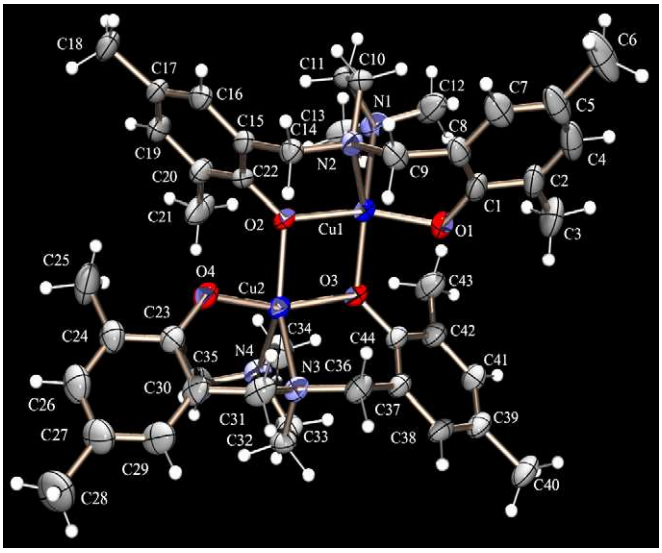

Fig. 2. ORTEP diagram (30% probability) of **I** with the atom numbering scheme.

The coordination geometry about the Cu-centers in both polymorphs can be best described as distorted square pyramidal with one phenolate oxygen, one amine nitrogen and two bridging oxygen atoms [N2, O1, O2, O3 around Cu1 and O4, N3,O3,O2 around Cu2 in **I**; O1, N2, O2, O2* (* = $x, 3/2-y, -z$) around Cu1 in **II**] defining the basal plane; the remaining amine N atoms N1, N4 in **I** and N1 in **II** occupy the apical sites. The displacement of the metal center towards the axial N atom from the least-squares plane through the basal atoms are 0.322(1) and 0.314(1) Å for Cu1 and Cu2 in **I** and 0.3146(2) Å for Cu1 in **II**. The dihedral angle of 63.74(12)°

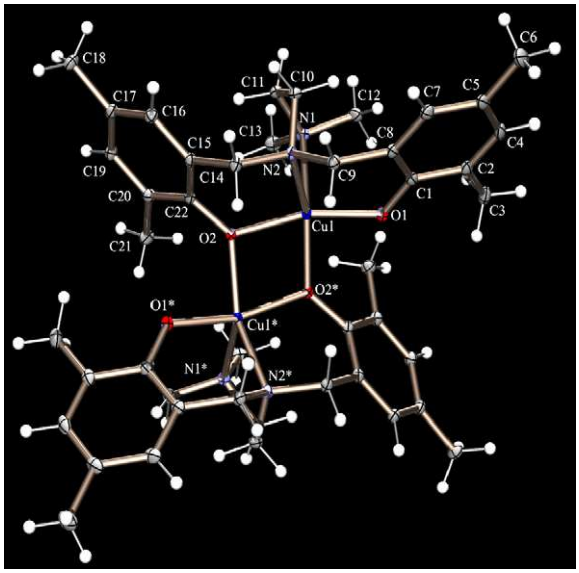

Fig. 3. ORTEP diagram (30% probability) of **II** with the atom numbering scheme.

between the two basal planes in **I** indicates a *syn-clinial* arrangement. The trigonality index parameter τ [$=(\phi_1-\phi_2)/60$, where ϕ_1 and ϕ_2 are the two largest L-M-L angles of the coordination sphere] has been calculated for the pentadentate copper sites [18,19]. The τ values of 0.25 and 0.13 for Cu1 and Cu2, respectively, in **I** indicate a different degree of distortion of the two metal sites (for a perfect square pyramid $\tau = 0$ and for a perfect trigonal bipyramid $\tau = 1$). In **II** the τ parameter for Cu1 is 0.24.

The Cu–O bond distances in the two polymorphs, lying in the range 1.866(3)–2.016(3) Å, are in agreement with that reported for analogous copper(II) systems [20–22]. The Cu–N (equatorial) bond lengths in **I** and **II**, ranging between 2.059(1) and 2.072(3) Å, are consistent with the corresponding values for similar Cu^{II}-diamine complexes [20–22]. The shortening of the Cu–N (equatorial) bond lengths [2.072(3)–2.078(3) Å in **I**, and 2.059(1) Å in **II**] in comparison to the Cu–N (axial) distances [2.352(3)–2.377(3) Å] is typical for a d^9 configuration of the Cu^{II} ion. The intramolecular Cu···Cu separations in the two polymers [2.950(1) and 3.007(1) Å] fall within the range of known Cu···Cu distances in double-bridged copper polynuclear systems [20–22]. The Cu1··O2··Cu2 angle is 96.76° and Cu1··O3··Cu2 is 96.24° for **I** and the Cu1··O2···Cu1 angle is 99.33° for **II**.

Both polymorphs exhibit a similar type of intramolecular C–H··· (arene) hydrogen bond (Table 2) involving the ethylene H- atoms and terminal phenyl rings, which influence the overall molecular conformations. In **I**, besides the intramolecular C–H··· interactions, there exists an additional intermolecular C–H··· interaction (Table 3), through which the individual dinuclear entities self assemble in the form of helices along the crystallographic *b*-axis (Fig. 4). The inherently curved nature of the dinuclear entities facilitates this helical assembly in which successive units of opposite curvature are united by CH···π interactions. The pitch of the helix is 15.33 Å. Adjacent helices are arranged in such a way that a central helix is surrounded by six other helices (Fig. 5).

The packing of the dinuclear units in **II** is also in the form of a helix, but now there are no intermolecular CH···π interactions, instead only weak van der Waals interactions leading to the association of successive units. The axis of the helix now is the crystallographic *a*-axis (Fig. 6). Inherently, the curved nature of the dinuclear entities facilitates this helical assembly in which successive units of opposite curvature stand up around a common axis. The pitch of the helix is 12.65 Å. Three-dimensional packing of these helices again is in the form of a hexagon, in which a central helix is flanked by six other helices (Fig. 7).

3.2. Heterogeneous catalysis

From the small angle powder diffraction patterns of **HMS** and **HMS-Cu-I** (SUP Fig. 1) it is clear that all four planes (100, 110, 200 and 210) of the 2D-hexagonal mesophase of **HMS** have been retained in **HMS-Cu-I**. BET surface areas and mesopore volumes for **HMS** and **HMS-Cu-I** are 1438 m^2g^{-1} and 0.93 ccg^{-1}; 976 m^2g^{-1} and 0.65 ccg^{-1}, respectively. The peak pore diameters for these two samples employing BJH pore size distribution are 2.8 and 2.1 nm, respectively. The decrease in surface area, pore diameter and pore volume of HMS after the loading of the Cu complex suggests that the metal complex has occupied the internal channel of the mesopores and is distributed uniformly inside the mesoporous channels, which is essential for utilizing the high surface area of the mesoporous host in liquid phase partial oxidation reactions.

In Table 4, the results of the catalytic activity of complex **I** immobilized over silica surfaces, **HMS-Cu-I,** are shown. Acetonitrile has been used as the solvent in all these liquid phase reactions. The major products for the partial oxidation of both styrene and cyclohexene were their respective epoxides. In Fig. 8, the time-on-stream for the conversion and epoxide selectivities in these reactions are plotted. It is clear from the figure that the selectivity of the epoxide for both substrates was high at the initial stage of the reaction. However, with time as the conversions reach

Table 2
Selected intramolecular contacts (Å, °) for polymorphs **I** and **II**.

D–H···A	D–H	H···A	D···A	D–H···A
I				
C11–H11A···Cg9	0.970	2.84	3.645(4)	149
C33–H33A···Cg11	0.970	2.86	3.730(5)	150
II				
C11–H11A···Cg6	0.955	2.69(2)	3.556(2)	150

Table 3
The intermolecular C–H···π contacts (Å, °) in polymorph **I**.

D–H···A	D–H	H···A	D···A	D–H···A
I				
C10–H10B···Cg10	0.969	2.90	3.645(5)	135

In polymorph **I**: Cg9 = C15–C16–C17–C19–C20–C22, Cg10 = C23–C24–C26–C27–C29–C30, Cg11 = C37–C38–C39–C41–C42–C44
In polymorph **II**: Cg6 = C15–C16–C17–C19–C20–C22

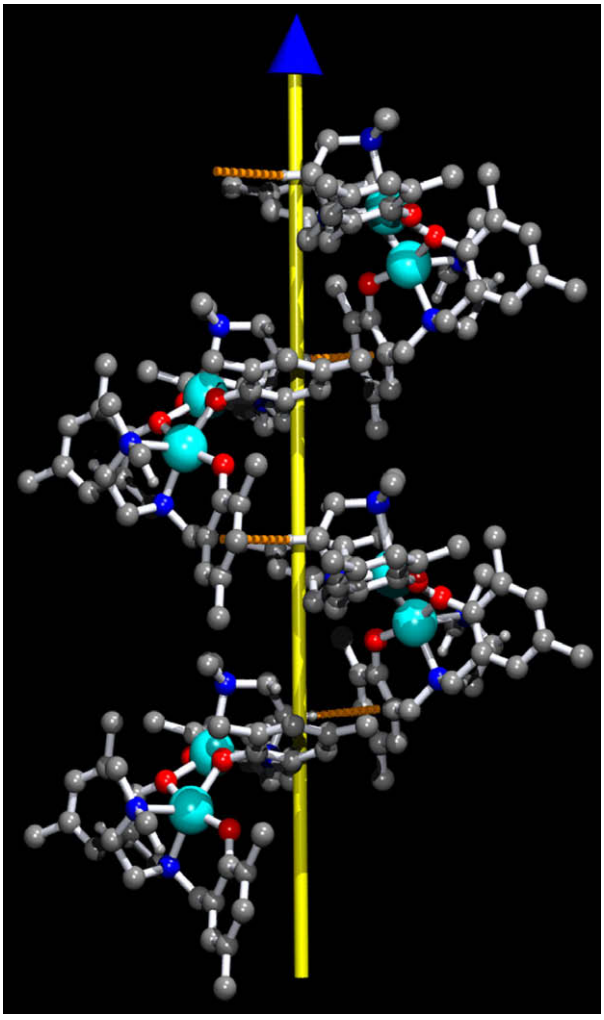

Fig. 4. Helical arrangement of the dinuclear units through C–H···π interactions in **I**.

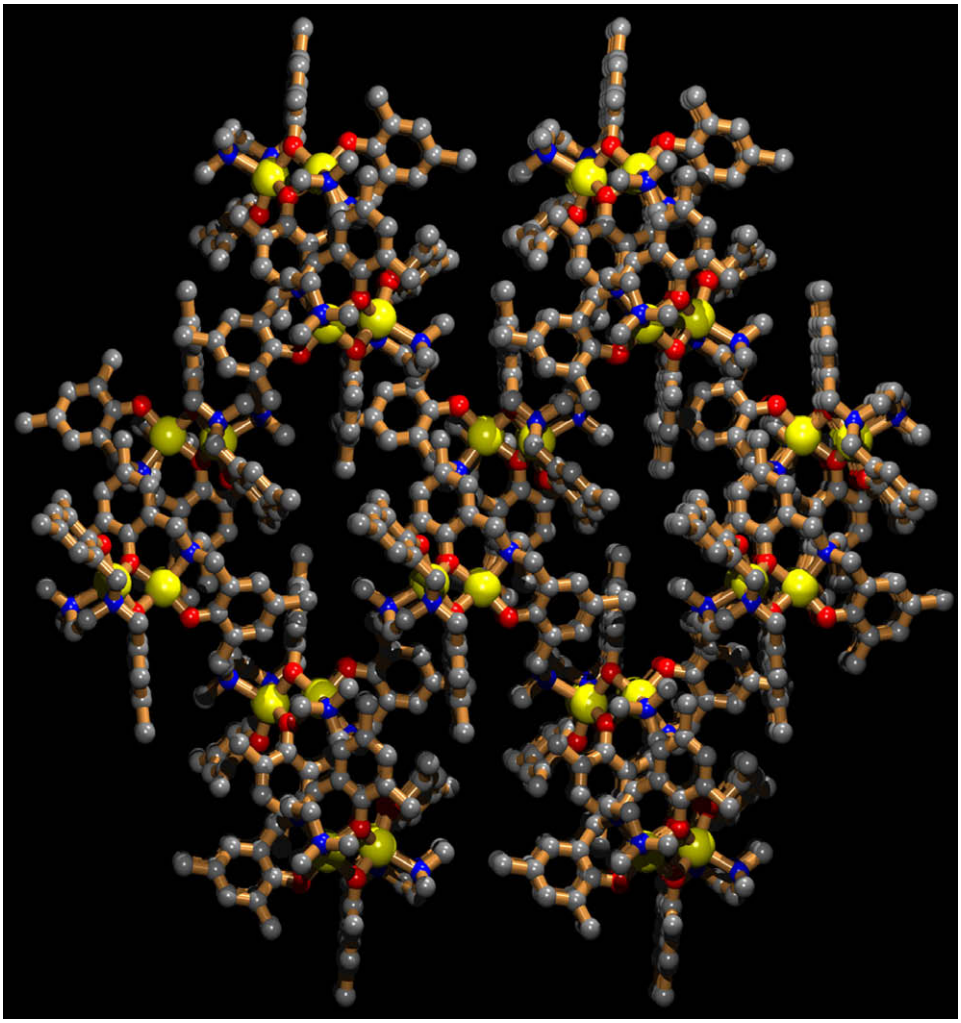

Fig. 5. Molecular packing in **I** viewed along the *a*-axis, revealing the hexagonal array of helices.

the respective maximums, the epoxide selectivities go down to some extent. This could be attributed to the hydrolysis of the epoxides to the respective diols, which is quite common for the liquid phase partial oxidation of olefins over a heterogeneous catalyst [10], as water coming from the oxidant in the reaction mixture promotes the epoxide ring opening. In Table 4, the TOF (turn over frequency) for different catalytic runs are also given. The TOF for cyclohexene conversion was relatively more than that for styrene. The immobilized catalyst shows moderately high TOFs for both the substrates. In order to show the superiority of the heterogeneous catalysts over the homogeneous ones, these reactions were carried out under homogeneous conditions and it was observed that the TOFs were found to be very poor (Table 4). These results suggest that the immobilization of complex **1** in the mesoporous matrix drastically enhances the catalytic activity. Nevertheless, the relatively high TOFs for the oxidation of styrene and cyclohexene suggest high catalytic efficiency for the Cu-hydroperoxo species that could form at the active sites in the presence of the TBHP oxidant [10]. For both the substrates the corresponding diols are the other major products. Hydrophobic aromatic ligands attached to the Cu-centers in the immobilized catalyst could provide the affinity towards the olefinic substrates. This may facilitate the adsorption of the substrates near the vicinity of the active sites and their subsequent oxidations. This could be responsible for high TOFs in these partial oxidation reactions.

3.3. Low temperature magnetic studies

The magnetic susceptibility of complex **I** was measured at 0.5*T* in the temperature range 2–300 K, and this is shown in Fig. 9. At 300 K, the $_{m}T$ value of 0.412 $cm^3\,Kmol^{-1}$ is significantly smaller than the expected value for two uncoupled Cu(II) ions. On lowering the temperature $_{m}T$ undergoes a monotonic decrease down to 80 K, suggestive of strong antiferromagnetic interactions operating. Below this temperature the $_{m}T$ value shows a constant non-zero value which may be due unaccounted background noise, as due to the strong antiferromagnetic nature we expect a zero $_{m}T$ value in this region. The magnetic data were properly fitted using the Bleaney–Bowers Eq. (1), derived from an isotropic exchange Hamiltonian $H = -JS_1 \cdot S_2$, and considering a small amount of non-coupled Cu(II) species (ρ).

$$\chi_m = (1-\rho)(2Ng^2\beta^2/kT)/[3+\exp(-J/kT)] + \rho(Ng^2\beta^2/2kT) \quad (1)$$

A best fit gives magnetic parameters of $g = 2.07$, $J = -341\ cm^{-1}$ and $\rho = 0.06$. The large negative J value indicates that the strong antiferromagnetic interactions are transmitted between Cu spins via the phenoxide linkage. The magnitude of the magnetic exchange coupling constant falls into the usual range of hydroxo-bridged Cu(II) dimers [23–25]. As depicted in SUP Fig. 2, the field dependence of the magnetization shows that the experimental magnetization value of 0.093 Nβ at 7 T is significantly lower that

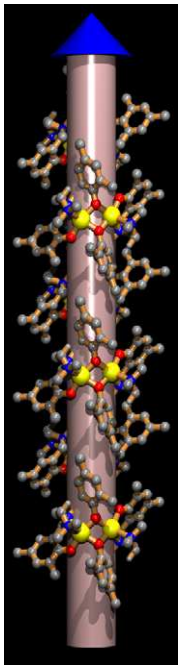

Fig. 6. Helical arrangement of dinuclear units through van der Waals interactions in **II**.

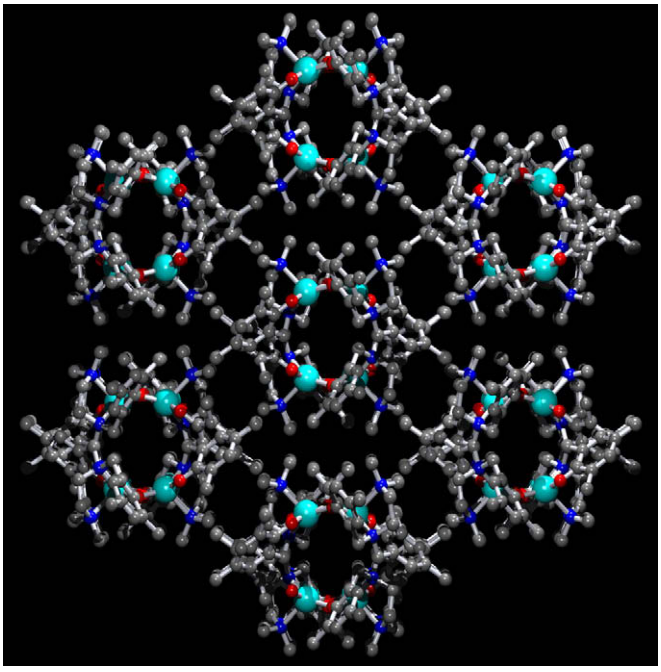

Fig. 7. Packing of helical units in **II** viewed along the *b*-axis.

the theoretical value (2.04 Nβ per Cu_2), confirming the presence of strong antiferromagnetic coupling between the Cu(II) ions through the phenoxide bridges.

3.4. Magneto-structural correlation

It is well known that the magnetic behavior of divalent copper complexes bridged equatorially by a pair of hydroxide [23–25], alkoxide [26,27] or phenoxide [28–38] oxygen atoms is highly dependent on the Cu–O–Cu bridge angle. Also it can be influenced

Table 4
Catalytic activity of **HMS-Cu-I** in the partial oxidation of olefins.[a]

Substrate	Time (h)	Conversion (%)	Epoxide (%)	Diol (%)	Others (%)	Turn over frequency (TOF)[b]
Styrene	12	89.4	63.2	16.9	19.9	48.0
Styrene[c]	12	4.2	15.5	81.4	3.1	
Styrene[d]	12	13.14	80.6	16.2	3.2	0.88
Cyclohexene	10	82.6	48.0	44.2	7.8	67.7
Cyclohexene[c]	12	1.6	4.8	84.5	10.7	
Cyclohexene[d]	12	34.81	22.6	72.1	5.3	2.96

[a] Reaction conditions: substrate 0.5 g; catalyst: **HMS-Cu-I**: 0.1 g, substrate: TBHP = 1:1; solvent: acetonitrile - 6 ml.
[b] TOF = moles of substrate converted per mole of Cu per h, Cu loading was estimated by AAS.
[c] Pure HMS was used as the catalyst.
[d] Pure Cu complex **I** (homogeneous) was used as catalyst.

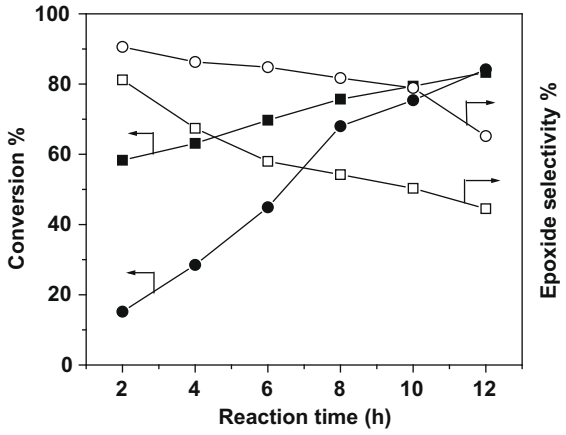

Fig. 8. Conversions of styrene (filled circle) and cyclohexene (filled square) for different reaction times in the liquid phase partial oxidation over **HMS-Cu-I**. Corresponding selectivities of styrene oxide (open circle) and cyclohexene oxide (open square) are at the right hand axis.

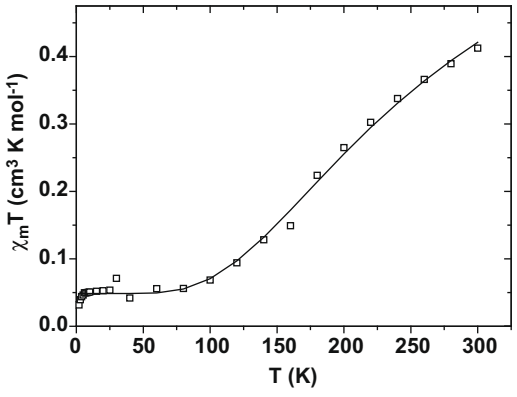

Fig. 9. Plot of $_{m}T$ versus T at 0.5T for **I**. The solid line gives a best fit with the modified Bleaney–Bowers equation.

to a smaller measure by the Cu–O (bridge) distance, the Cu···Cu separation, the geometry around the copper(II) centers and the geometry around the bridging oxygen atom. The magneto structural correlations in bis(μ-phenoxide)-bridged macrocyclic copper(II) complexes with flat dinuclear centers and no electronic perturbations have been studied [30], and a linear relationship between the exchange integral (J) and the phenoxide bridging angle (ϕ) of the form: $2J = -31.95\phi + 2462$ has been proposed. Using this

relationship a bridging angle of 96.76° for **I** leads to an expected 2*J* value of $-629.5\ cm^{-1}$, contrary to the experimental 2*J* value of $-341\ cm^{-1}$. This is probably due to the many other factors affecting the 2*J* values, especially the non-flat nature of the dinuclear unit in the present case.

3.5. Study of polymorphism

The gross composition of the complexes has been determined via elemental analysis, which is consistent with the single-crystal X-ray study. Qualitatively, the physical differences of the two polymorphs are revealed in their color, shape and melting points. The synthetic method was both reliable and predictable as under repeated crystallization experiment two polymorphs could concurrently be obtained. It is interesting that though the polymorphs are concomitant in nature due to kinetic factors, complex **I** appeared more quickly (within 2 days), on the upper part of the vessel when there was no trace of the complex **II**, and could be collected easily. With the gradual evaporation of the reaction mixture and increasing concentration of the solution, growth of complex **I** was inhibited and complex **II** was favored, and this complex appeared in the lower part of the vessel. This provided an easy way of isolating the two polymorphs. It is to be noted that when the crystallization experiment was conducted at relatively low temperature only complex **II** was favored, indicating the temperature sensitivity of the nucleation processes.

As mentioned earlier, complexes **I** and **II** are concomitant polymorphs of each other. Concomitant polymorphs arise when a material crystallizes in two or more forms out of the same reaction mixture [39]. It is also the subtlest and most challenging type of polymorphism, as screening out different crystal forms is often difficult. We were lucky that the two polymorphic forms could easily be separated as the crystals of polymorph **II** have been obtained at the later stage of the crystallization. The densities of complexes **I** and **II** are 1.268 and 1.337 g/cm^3, respectively, and according to the well known 'density rule', [39] the polymorph **II** with the higher density is most likely to be more stable and should appear latter. This is consistent with the fact that crystals of polymorph **II** have been obtained at the later stage of crystallization. Melting point determination provides a convenient means of assessing the relative stabilities of the different polymorphic forms of a substance [40–44]. Accordingly, attempts have taken to carry out DSC measurements to investigate melting behavior of complexes **I** and **II** (SUP. Fig. 3). The solid-state reaction corresponds to the large endothermic peak in the regions of 253 and 258 °C for **I** and **II,** respectively, which shows sharp mass loss in the TGA curves, indicating that the melting points of the two polymorphs are slightly different. In the case of **I**, an additional small endothermic peak at temperature 197 °C is observed, indicating the fact that it is stable up to 197 °C and after this temperature a phase transition occurs [45].

4. Conclusions

Using established crystal engineering methodologies we have been able to synthesize two dinuclear Cu(II)-bisphenolate complexes having interesting functional properties. The complexes are concomitant polymorphs and the X-ray crystal structure determination reveals the versatility of the self-assembly phenomena in which the weak interactions such as C–H···π and van der Waals forces crucially determine the molecular packing within the crystal, giving rise to two different modes of self-assembly and consequently two concomitant polymorphs. The strong antiferromagnetic property of the polymorph **I** strongly correlates with the crystal structure. The efficient heterogeneous catalytic activity of the copper(II) complex **1**, due to immobilization on a 2D-hexagonal mesoporous silica, in the liquid phase partial oxidation of olefins to epoxide in the presence of TBHP as an oxidant is noteworthy. We have confined our studies to complex **I**, as the complexes **I** and **II** differ from each other only by weak non-covanent interactions, and they are expected to behave identically, particularly in solution.

Acknowledgements

M.A. gratefully acknowledges the financial assistances from the DST (Ref. No. SR/S1/IC-35/2006), and CSIR (Ref. No. 01(7329)/07/EMR-II), New Delhi, India. M.A. also thanks to Dr. S. Das, School of Chemistry, University of Hyderabad, Hyderabad 500 046, India for X-ray data collection on complex **I**. M.N. thanks CSIR, New Delhi for a Senior Research Fellowship. A.B. wishes to thank DST, New Delhi for a Ramanna Fellowship Grant.

Appendix A. Supplementary data

CCDC 612752 and 612753 contain the supplementary crystallographic data for this article. These data can be obtained free of charge via http://www.ccdc.cam.ac.uk/conts/retrieving.html, or from the Cambridge Crystallographic Data Centre, 12 Union Road, Cambridge CB2 1EZ, UK; fax: (+44) 1223 336 033; or e-mail: deposit@ccdc.cam.ac.uk. Supplementary data associated with this article can be found, in the online version, at doi:10.1016/j.poly.2008.12.047.

References

[1] P. Chaudhuri, M. Hess, U. Flörke, K. Wieghardt, Angew. Chem., Int. Ed. Engl. 37 (1998) 2217.
[2] P. Chaudhuri, M. Hess, T. Weyhermüller, K. Wieghardt, Angew. Chem., Int. Ed. Engl. 38 (1999) 1095.
[3] P. Chaudhuri, M. Hess, J. Müller, K. Hildenbrand, E. Bill, T. Weyhermüller, K. Wieghardt, J. Am. Chem. Soc. 121 (1999) 9599.
[4] Y. Wang, J.L. DuBois, K.O. Hodgson, T.D.P. Stack, Science 279 (1998) 537.
[5] S. Itoh, M. Taki, S. Takayama, S. Nagatomo, T. Kitagawa, N. Sakurada, R. Arakawa, S. Fukuzumi, Angew. Chem., Int. Ed. Engl. 38 (1999) 2774.
[6] F. Thomas, G. Gelbon, I.G. Luneau, E.S. Aman, J.-L. Pierre, Angew. Chem., Int. Ed. Engl. 41 (2002) 3047.
[7] T.K. Paine, T. Weyhermüller, K. Wieghardt, P. Chaudhuri, J. Chem. Soc., Dalton Trans. (2004) 2092.
[8] A.R. Silva, K. Wilson, A.C. Whitwood, J.H. Clark, C. Freire, Eur. J. Inorg. Chem. (2006) 1275.
[9] S. Mukherjee, S. Samanta, A. Bhaumik, B.C. Roy, Appl. Catal. B Environ. 68 (2006) 12.
[10] S. Samanta, N.K. Mal, A. Bhaumik, J. Mol. Catal. A Chem. 236 (2005) 7.
[11] M. Hirotsu, M. Kojima, Y. Yoshikawa, Bull. Chem. Soc. Jpn. 70 (1997) 649.
[12] D. Chandra, N.K. Mal, M. Mukherjee, A. Bhaumik, J. Solid State Chem. 179 (2006) 1802.
[13] Software for the CCD Detector System, Bruker Analytical X-ray Systems Inc., Madison, WI, 1998.
[14] G.M. Sheldrick, SADABS, A Program for Absorption Correction with the Siemens SMART.
[15] G.M. Sheldrick, SHELXS-97, A Program for Solution of Crystal Structures, University of Göttingen, Germany, 1997.
[16] G.M. Sheldrick, SHELXL-97, A Program for Refinement of Crystal Structures, University of Göttingen, Germany, 1997.
[17] K. Kabsch, J. Appl. Crystallogr. 21 (1988) 916.
[18] M. Ali, A. Ray, W.S. Sheldrick, H. Mayer-Figge, S. Gao, A.I. Sahmes, New J. Chem. 28 (2004) 412.
[19] A.W. Addision, T.N. Rao, J. Reedijk, J. van Rijn, G.C. Verschoor, J. Chem. Soc., Dalton Trans. (1984) 1349.
[20] H. Saimiya, Y. Sunatsuki, M. Kojima, S. Kashino, T. Kambe, M. Hirotsu, H. Akashi, K. Nakajima, T. Tokii, J. Chem. Soc., Dalton Trans. (2002) 3737.
[21] D.G. Lonnon, S.B. Colbran, D.C. Craig, Eur. J. Inorg. Chem. (2006) 1190.
[22] S. Wang, Z. Pang, K.D.L. Smith, Inorg. Chem. 32 (1993) 4992.
[23] V.H. Crawford, H.W. Richardson, J.R. Wasson, D.J. Hodgson, W.E. Hatfield, Inorg. Chem. 15 (1976) 2107.
[24] D.J. Hodgson, Prog. Inorg. Chem. 19 (1975) 173;
A. Asokan, B. Varghese, P.T. Manoharan, Inorg. Chem. 38 (1999) 4393.
[25] M.F. Charlot, S. Jeannin, O. Kahn, J. Licrece-Abaul, J. Martin-Freere, Inorg. Chem. 18 (1979) 1675.

[26] M. Handa, N. Koga, S. Kida, Bull. Chem. Soc. Jpn. 61 (1988) 3853.
[27] M. Kodera, N. Terasako, T. Kita, Y. Tachi, K. Kano, M. Yamazaki, M. Koikawa, T. Tokii, Inorg. Chem. 36 (1997) 3861.
[28] R. Gupta, S. Mukherjee, R. Mukherjee, J. Chem. Soc., Dalton Trans. (1999) 4025.
[29] S.K. Dutta, U. Flörke, S. Mohanta, K. Nag, Inorg. Chem. 37 (1998) 5029.
[30] L.K. Thompson, S.K. Mandal, S.S. Tandon, J.N. Bridson, M.K. Park, Inorg. Chem. 35 (1996) 3117.
[31] H. Adams, N.A. Bailey, I.K. Campbell, D.E. Fenton, Q.-Y. He, J. Chem. Soc., Dalton Trans. (1996) 2233.
[32] D. Block, A.J. Blake, K.P. Dancey, A. Harrison, M. McPatlin, S. Parsons, P.A. Tasker, G. Whitlaker, M. Schröder, J. Chem. Soc., Dalton Trans. (1998) 3953.
[33] Y. Sunatsuki, M. Nakamura, N. Matsumoto, F. Kai, Bull. Chem. Soc. Jpn. 70 (1997) 1851.
[34] M. Vaidyatham, R. Viswanathan, M. Palaniandavar, T. Balasubramanian, P. Prabhaharan, T.P. Muthiah, Inorg. Chem. 37 (1998) 6418.
[35] N.R. Sangeetha, K. Baradi, R. Gupta, C.K. Pal, V. Manivannan, S. Pal, Polyhedron 18 (1999) 1425.
[36] J. Galy, J. Jaud, O. Kahn, P. Tola, Inorg. Chim. Acta 36 (1979) 229.
[37] S.S. Tandon, L.K. Thompson, J.N. Bridson, Inorg. Chem. 32 (1993) 32.
[38] Y. Xie, H. Jiang, A.S.C. Chan, Q. Liu, X. Xu, C. Du, Y. Zhu, Inorg. Chim. Acta 333 (2002) 138.
[39] J. Bernstein, R.J. Davey, J.-O. Henck, Angew. Chem., Int. Ed. 38 (1999) 3441.
[40] J. Bernstein, Polymorphism in Molecular Crystals, Oxford University Press, Oxford, 2002.
[41] A. Burger, R. Ramberger, Mikrochim. Acta 2 (1979) 259.
[42] A. Burger, R. Ramberger, Mikrochim. Acta 2 (1979) 273.
[43] D. Giron, Thermochim. Acta 248 (1995) 1.
[44] L. Yu, J. Huang, K.J. Jones, J. Phys. Chem. B 109 (2005) 19915.
[45] D.V. Soldatov, A.T. Henegouwen, G.D. Enright, C.I. Ratcliffe, J.A. Ripmeester, Inorg. Chem. 40 (2001) 1626.